Mirabilite and heptahydrate characterization from infrared microscopy and thermal data

Conference Paper · October 2012

CITATIONS
3

READS
400

5 authors, including:

Ronan L Hébert
CY Cergy Paris Université
90 PUBLICATIONS **1,947** CITATIONS
SEE PROFILE

Ann Bourgès
Ministère de la culture et de la communication
30 PUBLICATIONS **406** CITATIONS
SEE PROFILE

Beatriz Menéndez
CY Cergy Paris University
90 PUBLICATIONS **3,033** CITATIONS
SEE PROFILE

12th International Congress on the Deterioration and Conservation of Stone
Columbia University, New York, 2012

MIRABILITE AND HEPTAHYDRATE CHARACTERIZATION FROM INFRARED MICROSCOPY AND THERMAL DATA.

Mélanie Denecker,[1] Ronan Hébert,[1], Ann Bourgès,[2] Beatriz Menendez[1] and Eric Doehne[3]
[1]*Géosciences et Environnement Cergy, Université de Cergy-Pontoise, F-95031 Cergy-Pontoise cedex. Contact author: melanie.denecker@u-cergy.fr*
[2]*Laboratoire de Recherche des Monuments Historiques (LRMH), 29 rue de Paris, 77420 Champs sur Marne, France*
[3]*Conservation Sciences, Pasadena, CA, USA*

Abstract

Sodium sulfate is widely regarded as the most damaging salt for porous building materials. To understand this complex and incompletely understood phenomena, it is important to predict which phases will crystallize under a range of environmental conditions and which phase transitions will cause damage. In this study we present data on the crystallization of mirabilite and heptahydrate from infrared microscopy and temperature data.

This work documents the crystalline phases and their transitions under controlled environmental conditions (temperature and relative humidity, RH). The different phases in a droplet of sodium sulfate solution (28 and 30 Na2SO4 wt%) are observed using FTIR-ATR spectroscopy. As heptahydrate contains less H2O molecules than mirabilite, the H_2O absorption band enables the distinction between these two phases.

The temperature data are acquired using a thermocouple in a solution of sodium sulfate (28 and 30 Na2SO4 wt%) that is cooled from 40°C to 5°C. As the temperature decreases, a series crystallization events are recorded though the temperature profile. According to these experiments, heptahydrate crystallizes more easily than mirabilite.

The importance of environmental conditions and the protocol establishment are discussed. The approach of these methods helps us to understand the crystallization sequence of sodium sulfates and later better apprehend the damage of building stone.

Keywords: Sodium sulfate, crystallization, FTIR-ATR spectroscopy, thermocouple

1. Introduction

Sodium sulfate attack is one of the most damaging decay phenomena for building stone. The main damage results from the cyclic crystallization of salts in pores (Goudie and Viles 1997), especially hydrated salt phases which crystallize rapidly at a high supersaturation (Rodriguez-Navarro et al 2000; Tsui et al 2003; Steiger and Asmussen 2003; Flatt 2002). The study of sodium sulfate crystallization ultimately aims at preventing salt deterioration of important building materials in order to improve the conservation of cultural heritage and also any kind of construction.

Sodium sulfates occur as several phases: the decahydrate (mirabilite Na_2SO_4-$10H_2O$) and the anhydrous (thenardite Na_2SO_4) phases crystallize under normal ambient conditions. A second metastable hydrate (heptahydrate, Na_2SO_4-$7H_2O$) was noted in the middle of the 19th (Loewel 1850) and is metastable. Several studies (Loewel 1850; de Coppet 1901; Hartley et al. 1908) showed that heptahydrate crystallizes first from

solution during cooling of a bulk solution, rather than mirabilite. The heptahydrate phase can be obtained either by cooling a sodium sulfate solution (Hamilton and Hall 2008; Derluyn et al 2010) or a material whose pores are saturated with a sodium sulfate solution (Rijniers et al 2005; Hamilton and Hall 2008; Hamilton et al 2008; Espinosa-Marzal and Scherer 2008).

In the present study we perform temperature cycles on sodium sulfates solutions under conditions in closed system in order to crystallize heptahydrate. During these cycles we record the temperature of the solution in order to observe exo and/or endo thermic reactions that are linked to important phase transitions. We also use Fourier Transform Infrared Attenuated Total Reflection (FTIR-ATR) in order to investigate the crystallization changes of droplets during cooling of solutions with different concentrations.

In the following section, the experimental approaches by FTIR-ATR and thermal monitoring are described. Then the experimental results for each method are discussed and the importance of environmental conditions and testing protocols are emphasized.

2. Experimental approaches

2.1 Material

Na_2SO_4 solutions with 30 and 28 Na2SO4 wt% concentrations are prepared using anhydrous Na_2SO_4 (Natriumsulfat ROTH, ≥ 99.0 %) dissolved in demineralized water at 60°C. Droplets of about ≈ 100 µl are used in the case of FTIR-ATR spectroscopy, whilst we used volumes of 30 ml of solution for the thermal monitoring.

2.2 FTIR-ATR spectroscopy

FTIR spectra were measured using a Perkin-Elmer, Spectrum 100 FTIR equipped with a microscope spectrum Spotlight 400 FTIR imaging system. Each spectrum was recorded from the accumulation of 10 scans from a droplet set on the ATR crystal. Spectra were acquired in the wavenumber interval of 530-4000 cm^{-1} with a spectral resolution of 4 cm^{-1}.

All measurements were made at 55% ± 3% of relative humidity (RH) corresponding to the RH room. A transparent window of CaF_2 was placed on the sample to create a contact between the ATR crystal and the droplet, and to isolate the sample (fig 1).

The experimental procedure consists in placing a droplet (at 65°C) directly on the ATR platinum previously cooled with ice for 3 minutes. The spectra were recorded immediately after the deposition of the droplet on the ATR surface. After 20 minutes, the sample is heated with a hairdryer in order to favor the crystallization of thenardite.

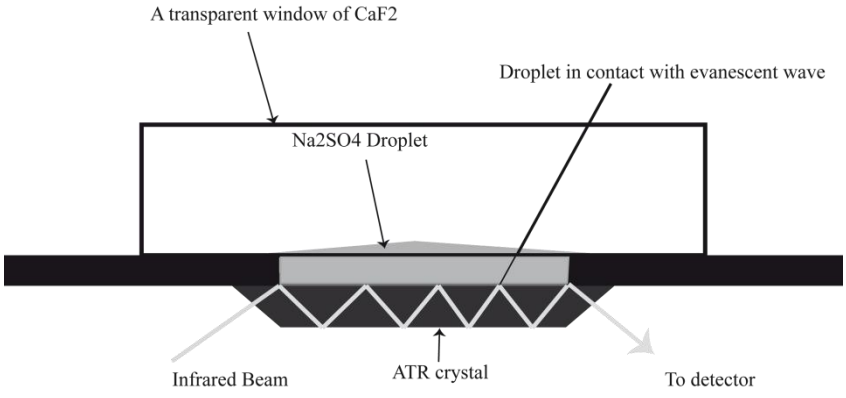

Figure 1. Protocol device used for FTIR-ATR spectroscopy. Droplet is confined between a transparent window of CaF_2 and the ATR crystal.

2.3 Thermal monitoring

A series of five temperature cycles were performed using a climatic test chamber Binder MKF with program control. The temperature range of the climatic chamber is -40°C up to 180°C with an accuracy of ± 1.0°C, and the RH range is between 10% and 98% RH with a precision of ± 2.0 % RH. For these experiments RH was fixed and kept at 35 ± 2.0 % during the duration of the program.

The test is composed of cycles, which last 20 hours:

- 10h at 40°C followed by
- 10h at 5°C to allow the crystallization of hydrates (figure 2).

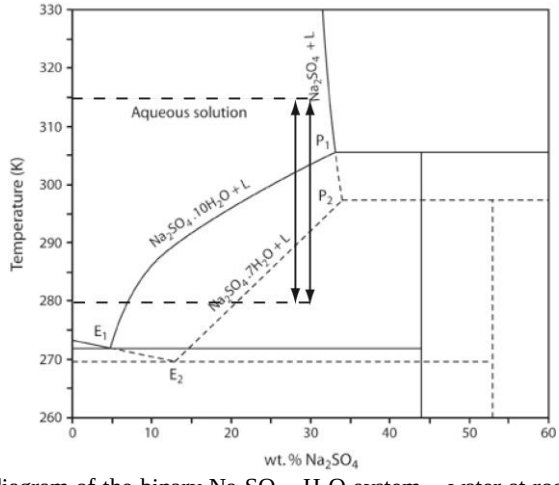

Figure 2. Phase diagram of the binary Na_2SO_4 - H_2O system – water at room pressure showing stable phase boundaries (black lines) and metastable phase boundaries (dashed lines). After Negi and Anand (1985) with solubility data tabulated in Garrett (2001); Brand 2009. The measured concentration of Na_2SO_4 solution for temperature cycles with 28 and 30 Na_2SO_4 wt % are indicated. The solution is cooled down from 40°C to 5°C via the heptahydrate. solubility line.

The temperature change from 40°C to 5°C and reversely was abrupt (within a 1 sec). These cycles were performed only on solutions in closed system (figure 3). The temperature was recorded with a precision of ± 0.1°C via a type K thermocouple which was put in the solution. The temperature was registered every 5 sec using an Agilent data logger.

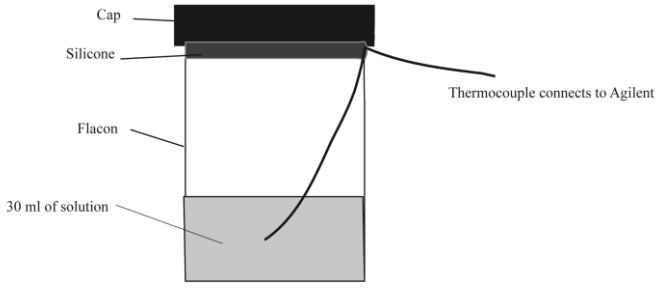

Figure 3. Schematic of the setup used for thermal monitoring. The thermocouple dips into 30 ml of solution. A silicon sealant joint is dispatched around the cap in order to obtain the best possible confinement of the sodium sulfate solutions

3. Results and Discussion

3.1 Crystallization of Na_2SO_4 droplets

Figure 4 shows examples of FTIR-ATR spectra from a droplet with a 30 Na_2SO_4 wt% concentration. Each spectrum corresponds to an average spectrum from the accumulation of multiple spectra sampled in a given surface. The response is characteristic to each component of the sample studied.

The absorption in the regions 3650-3100 cm^{-1} and 1575-1700 cm^{-1} show the presence of – OH bond (Weiss 1969) whilst those at 1000-1300 cm^{-1} (Durie and Milne 1978; Tong et al 2010) and 580-670 cm^{-1} (Weiss 1969) correspond to the part of -SO_4^{2-} bonds, respectively ν_2-SO_4^{2-} and ν_1-SO_4^{2-}. From t=0 to t=1 min, the vibration (ν) of –OH (ν-OH) band intensity increases and shifts from ≈ 3353 to 3396 cm^{-1}, and the ν_2-SO_4^{2-} band stays at 1085 cm^{-1}. After t=1min the ν-OH and ν_2-SO_4^{2-} bands intensity decrease and the latter shifts from ≈ 1085 to 1103 cm^{-1} when the droplet is heated. Although the spectra are distinguished one to another, their main features remain the same. The results using a solution with a concentration of 28 Na_2SO_4 wt% are not presented here because they are similar to the 30 Na_2SO_4 wt% concentration.

Figure 5a and 5b, respectively from 28 and 30 Na_2SO_4 wt% droplets, show the spectra evolution of crystals forming from a droplet at room temperature after different times of evaporation. Figure 5a indicates a decreasing of the ν-OH band intensity from t=0 to t=3h30 with a band moving from 3350 to 3422 cm^{-1}. The ν_1- SO_4^{2-} band intensity develops strongly at t=3h30. The ν_2-SO_4^{2-} band remains the same during all experiment. Figure 5b shows an increasing of the ν-OH band intensity from t=0 to t=2h with a band shift from 3345 to 3368 cm^{-1}. After t=2h, the ν-OH band intensity strongly decrease with a shift from 3368 to 3430 cm^{-1}. The ν_2-SO_4^{2-} band intensity increase during all

measurement, it moves from 1075 to 1093 cm^{-1} only between t=4 and t=6h. The ν_1-SO_4^{2-} band intensity develops strongly at t=4h.

The features remain the same for the two experiments with a decrease of the ν-OH band intensity. There is a significant change for the 30 Na_2SO_4 wt% droplet during the first step of the experiment

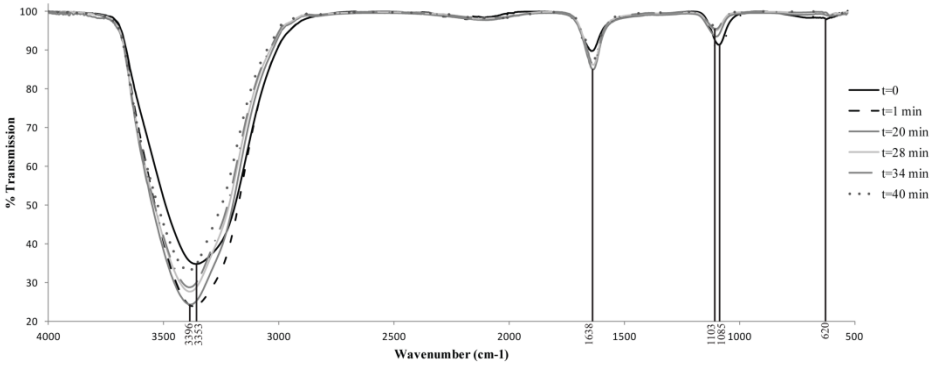

Figure 4. Infrared spectra of a droplet from the 30 Na_2SO_4 wt% solution versus wavenumber (cm^{-1}), under constant RH (room RH = 55% ± 2%). Measurements are performed on the cooled droplet from t=0 to t=20 min. Then the droplet is heated with hairdryer from t=28 to t=40 min.

.

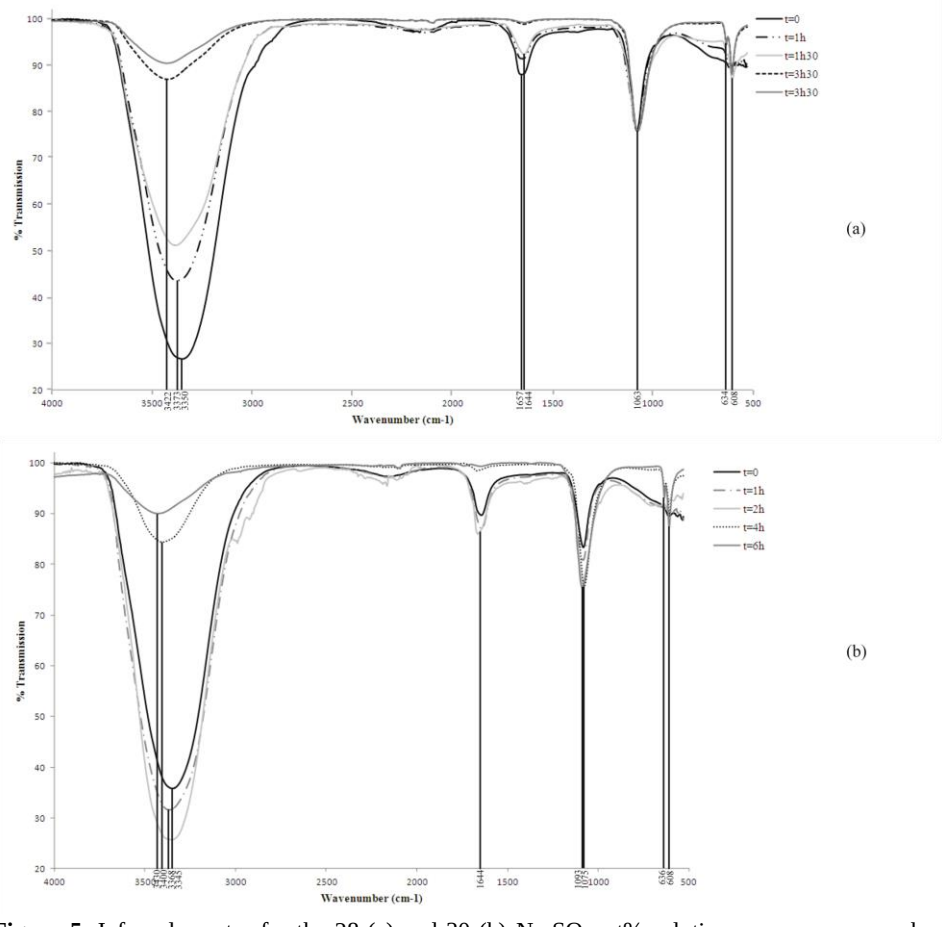

Figure 5. Infrared spectra for the 28 (a) and 30 (b) Na_2SO_4 wt% solutions versus wavenumber (cm^{-1}), under constant RH (room RH = 55% ± 2%). Measurements are from crystals forming in the droplet at room temperature (20°C ± 0.5°C). The t=0 curve corresponds to the precipitation of the first crystal. The crystal remains at room temperature during the experiment after precipitation.

3.2 Crystallization of Na_2SO_4 solutions

The results of the two experiments (i.e. with the two different concentrations) are presented in Figures 6a and 6b. Starting at a temperature T=40°C, after 10h, the solution is cooled down with a rate of 0.33°C/min until 5°C.

Temperature shows different profiles depending on the solution concentration. The first cycle of the 30 Na_2SO_4 wt% solution presents a small exothermic peak during the cooling at 6.94°C (figure 6a and 6b). It occurs only once. The heating rate is equal to 0.05°C/min on an interval time of 15.6 min. The other curve corresponding to the 28 Na_2SO_4 wt% solution shows exothermic peaks during the first two cycles: at 5.75°C and 5.84°C (figure 6a and 6b). The heating rates are equal to 0.02°C/min for the first cycle, and 0.01°C/min for the second with an interval time of 39 min and 32.4 min respectively.

The other cycles reveal slow temperature decrease. The heating rate is more pronounced during the first cycle, and decrease with time.

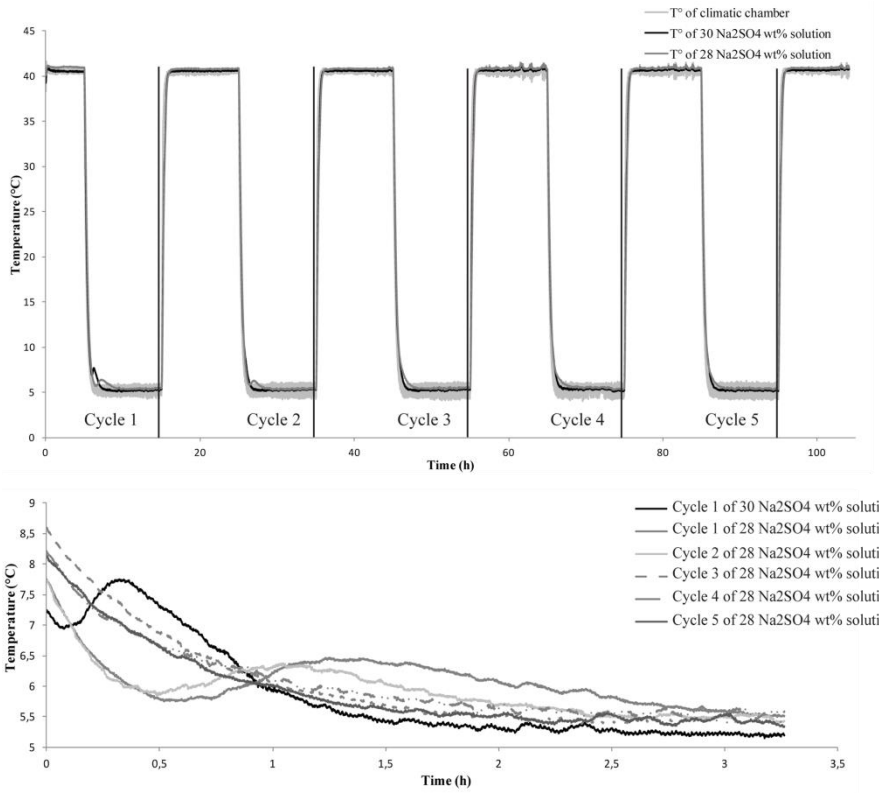

Figure 6. (a) Examples of temperature profiles from the climatic chamber (light gray), the 30 (black) and 28 (gray) Na_2SO_4 wt% solutions, versus time during temperature cycles (b) Focusing on the cooling periods of each cycle of the 28 Na_2SO_4 wt% solution (gray), and only the first cycle of the 30 Na_2SO_4 wt% solution (black).

3.3 Discussion

Both FTIR-ATR spectra for the 28 and 30 Na_2SO_4 wt% concentrations (figure 5a and 5b) indicate the formation of mirabilite at a RH= 55 ± 3% and T= 20 ± 0.5°C. During the droplet evaporation the mirabilite crystal transforms progressively into Na_2SO_4 anhydrous: the –OH band intensity decreases whereas the $-SO_4^{2-}$ band intensity increases or remains constant. The increase of ν-OH band of the 30 Na_2SO_4 wt% solution from t=0 to t=2h can be attributed to the transition phase between heptahydrate and mirabilite as the amount of OH increases (figure 5b). Concerning the cooled-drying cycle of the 30 Na_2SO_4 wt% droplet (figure 4), an increase of the ν-OH band is also observed. The ν-OH band increases during the first minute of the cooling droplet but

decreases afterwards. This phenomenon is also observed for the 28 Na_2SO_4 wt% solution. The position, width, and shape of the –OH bands of FTIR-ATR spectroscopy are affected by the salt ions (Max and Chapados 2001). The displacement and width variations of –OH bands can be assigned as a phase transition between two phases.

The exothermic peaks presented in figure 6a and 6b occur progressively and are not instantaneous as mirabilite crystallization according to Rodriguez-Navarro and Doehne (1999). These peaks could be attributed to heptahydrate formation. One must notice that only one peak on the temperature profile of 30 Na_2SO_4 wt% solution has been observed, compared to the other solution. It is likely that time and and/or temperature are not sufficient to dissolve all salt nuclei at 40°C. The intensity of the exothermic peaks of the 28 Na_2SO_4 wt% solution decreases progressively with temperature cycles until no exothermic peak is distinguishable. Nevertheless we can observe from cycle 3 to cycle 5 that the temperature decreases more slowly, which can result from a less important exothermic effect. This decreasing tendency can be slowed down by an exothermal effect. This may be similar to the problem of dissolving crystals at 40°C, since their amount increases from one cycle to another.

The importance of environmental conditions and the protocol are the two main conditions in the planning of experiments. A thermal monitoring and confinement cell to maintain temperature and RH can be used for the FTIR-ATR spectroscopy. Future work will consider ways to isolate crystals from the effects of the solution. Increasing the interval time at 40°C and/or the temperature to 50-60°C may help evaluate our hypothesis concerning the disappearance of the thermic peaks during cycles.

4. Conclusions

Sodium sulfate phase transitions have been characterized from droplets and solutions (with 28 and 30 Na_2SO_4 wt% concentration). The phase crystallizations are observed using the FTIR-ATR spectroscopy and thermal monitoring. The preliminary data confirm that heptahydrate formation occurs more easily from a solution close to supersaturation, and with cooling.

Acknowledgment

Mélanie Denecker is indebted to the Cergy-Pontoise University for financial support and the Laboratoire de Recherche des Monuments Historiques (LRMH) for access to analytical facilities. This research is part of the Patrima.org project.

References

Brand, H. (2009). Thermoelastic properties of salt hydrates and implication for geological structures. University College London. Thesis. 240

De Coppet, L.C. (1901). Sur l'heptahydrate de sulfate de sodium. Bull. Soc. Vaud. Sci. Nat. XXXVII 141, 455-462.

Derluyn, H., Saidov, T. A., Espinosa-Marzal, R. M., Pel, L., & Scherer, G. W. (2011). Sodium sulfate heptahydrate I: The growth of single crystals. *Journal of Crystal Growth*, *329*(1), 44-51.

Durie, R.A., Milne, J.W. (1978). Infrared spectra anhydrous alkali métal sulphates. Spectrochimica Acta, 34A, 215-220.

Espinosa Marzal, R. M., & Scherer, G. W. (2008). Crystallization of sodium sulfate salts in limestone. *Environmental Geology*, *56*(3-4), 605-621.

Flatt, R. J., & Scherer, G. W. (2002). Hydration and crystallization pressure of sodium sulfate: a critical review. *Materials Research Society Symposium Proceedings*, *712*(Materials Issues in Art and Archaeology VI), 30, 2001, Boston, Ma.

Garrett, D. E. (2001): *Sodium sulfate: handbook of deposits, processing, properties, and use.* Academic Press.

Goudie, A., Viles, H. (1997). Salt Weathering Hazards. Wiley, Chichester

Hamilton, A., & Hall, C. (2008). Sodium sulfate heptahydrate: a synchrotron energy-dispersive diffraction study of an elusive metastable hydrated salt. *Journal Of Analytical Atomic Spectrometry*, *23*(6), 840-844.

Hamilton, A., Hall, C., & Pel, L. (2008). Sodium sulfate heptahydrate: direct observation of crystallization in a porous material. *Journal of Physics D: Applied Physics*, *41*(21), 212002.

Hartley, H., Jones, B. M., Hutchinson, G. A., & Jones, G. (1908). The Spontaneous Crystallization of Sodium Sulfate Solutions. *Journal of the Chemical Society Transactions*, *433*(7021), 825-833.

Loewel, H. (1850). Observations sur la sursaturation des dissolutions salines. *Ann. Chim. Phys.*, *29*, 62–127.

Max, J.-J., & Chapados, C. (2001). IR spectroscopy of aqueous alkali halide solutions: Pure salt-solvated water spectra and hydration numbers. *The Journal of Chemical Physics*, *115*(6), 2664.

Negi, A. S., & S. C. Anand (1985): *A textbook of physical chemistry*. New Age Publishers. Orlando, T. M., T. B. McCord, & G. A. Grieves (2005): The chemical nature of Europa's surface material and the relation to a subsurface ocean. *Icarus* **177**(2), 528-533

Rijniers, L. A., Huinink, H. P., Pel, L., & Kopinga, K. (2005). Experimental evidence of crystallization pressure inside porous media. *Physical Review Letters*, *94*(7), 075503.

Rodriguez-Navarro, C., & Doehne, E. (1999). Salt weathering: influence of evaporation rate, supersaturation and crystallization pattern. *Earth Surface Processes and Landforms*, *24*(3), 191-209. John Wiley & Sons.

Rodriguez-navarro, C., Doehne, E., & Sebastian, E. (2000). How does sodium sulfate crystallize ? Implications for the decay and testing of building materials. *Cement and Concrete Research*, *30*(10), 1527-1534.

Steiger, M., & Asmussen, S. (2008). Crystallization of sodium sulfate phases in porous materials: The phase diagram Na2SO4-H2O and the generation of stress. *Geochimica et Cosmochimica Acta*, *72*(17), 4291-4306.

Tong, H.-J., Reid, J. P., Dong, J.-L., & Zhang, Y.-H. (2010). Observation of the crystallization and supersaturation of mixed component NaNO3-Na2SO4 droplets by FTIR-ATR and Raman spectroscopy. *The Journal of Physical Chemistry A*, *114*(46), 12237-12243.

Tsui, N., Flatt, R. J., & Scherer, G. W. (2003). Crystallization damage by sodium sulfate. (T. Takanami & G. Kitagawa, Eds.)*Journal of Cultural Heritage*, *4*(2), 109-115.

Weiss, P. (1969). Infrared spectroscopy. Its use in the coatings Industry. Infrared Spectroscopy Committee of the Chicago Society for Paint Technology, Federation of

Societies for Paint Technology, Philadelphia, 1969. X + 456 pp. 20.00 to members, 30.00 to nonmembers. *Journal of Applied Polymer Science*, *13*(11), 2509-2509.